



NAVAL POSTGRADUATE SCHOOL

MONTEREY, CALIFORNIA

THESIS

**AERODYNAMIC PREDICTIONS, COMPARISONS, AND
VALIDATIONS USING MISSILELAB AND MISSILE
DATCOM (97)**

by

Teo, Hoon Hong

December 2008

Thesis Advisor:

M. S. Chandrasekhara

Approved for public release; distribution is unlimited

THIS PAGE INTENTIONALLY LEFT BLANK

REPORT DOCUMENTATION PAGE			<i>Form Approved OMB No. 0704-0188</i>	
Public reporting burden for this collection of information is estimated to average 1 hour per response, including the time for reviewing instruction, searching existing data sources, gathering and maintaining the data needed, and completing and reviewing the collection of information. Send comments regarding this burden estimate or any other aspect of this collection of information, including suggestions for reducing this burden, to Washington headquarters Services, Directorate for Information Operations and Reports, 1215 Jefferson Davis Highway, Suite 1204, Arlington, VA 22202-4302, and to the Office of Management and Budget, Paperwork Reduction Project (0704-0188) Washington DC 20503.				
1. AGENCY USE ONLY (Leave blank)		2. REPORT DATE December 2008	3. REPORT TYPE AND DATES COVERED Masters' Thesis	
4. TITLE AND SUBTITLE Aerodynamic Predictions, Comparisons, and Validations Using MissileLab and Missile Datcom (97)			5. FUNDING NUMBERS	
6. AUTHOR(S) Teo, Hoon Hong				
7. PERFORMING ORGANIZATION NAME(S) AND ADDRESS(ES) Naval Postgraduate School Monterey, CA 93943-5000			8. PERFORMING ORGANIZATION REPORT NUMBER	
9. SPONSORING /MONITORING AGENCY NAME(S) AND ADDRESS(ES) N/A			10. SPONSORING/MONITORING AGENCY REPORT NUMBER	
11. SUPPLEMENTARY NOTES The views expressed in this thesis are those of the author and do not reflect the official policy or position of the Department of Defense or the U.S. Government.				
12a. DISTRIBUTION / AVAILABILITY STATEMENT Approved for public release; distribution is unlimited			12b. DISTRIBUTION CODE	
13. ABSTRACT (maximum 200 words) <p>Aerodynamic prediction software is often used in the early stages of missile systems designed to quickly and accurately estimate the aerodynamics of a wide variety of missile configuration designs operating over many different flight regimes. It is also possible to use these empirical packages to validate flight data collected from wind tunnel tests and other open sources. Analysis of such data provides users with insights to the performance of a particular missile system and if necessary, enables the development of an appropriate defense system.</p> <p>Wind tunnel test data on an SA-2 class missile modified by suitable modeling was provided by MSIC. For this Thesis, this data set became the bench-mark for validating the Missile Datcom (97) empirical code that was used to compute the performance of the missile. The missile geometry was modeled using the interface MissileLab. A series of simulations for different flight operating conditions was carried out. The primary quantities compared were the axial force coefficient, C_A and the skin friction coefficient, C_f. This Thesis describes the results obtained along with the geometry changes that became necessary to obtain reasonable agreement.</p>				
14. SUBJECT TERMS Missile Aerodynamics, Missile Datcom (97), MissileLab			15. NUMBER OF PAGES 51	
			16. PRICE CODE	
17. SECURITY CLASSIFICATION OF REPORT Unclassified	18. SECURITY CLASSIFICATION OF THIS PAGE Unclassified	19. SECURITY CLASSIFICATION OF ABSTRACT Unclassified	20. LIMITATION OF ABSTRACT UU	

THIS PAGE INTENTIONALLY LEFT BLANK

Approved for public release; distribution is unlimited

**AERODYNAMIC PREDICTIONS, COMPARISONS, AND VALIDATIONS
USING MISSILELAB AND MISSILE DATCOM (97)**

TEO, Hoon Hong
Major, Republic of Singapore Air Force
B.Eng., University of Manchester, Institute of Science and Technology, 2000

Submitted in partial fulfillment of the
requirements for the degree of

MASTER OF SCIENCE IN MECHANICAL ENGINEERING

from the

**NAVAL POSTGRADUATE SCHOOL
December 2008**

Author: TEO, Hoon Hong

Approved by: Prof. M. S. Chandrasekhara

Prof. Knox T. Millsaps
Chairman, Department of Mechanical and Astronautical
Engineering

THIS PAGE INTENTIONALLY LEFT BLANK

ABSTRACT

Aerodynamic prediction software is often used in the early stages of missile systems designed to quickly and accurately estimate the aerodynamics of a wide variety of missile configuration designs operating over many different flight regimes. It is also possible to use these empirical packages to validate flight data collected from wind tunnel tests and other open sources. Analysis of such data provides users with insights to the performance of a particular missile system and if necessary, enables the development of an appropriate defense system.

Wind tunnel test data on an SA-2 class missile modified by suitable modeling was provided by MSIC. For this Thesis, this data set became the bench-mark for validating the Missile Datcom (97) empirical code that was used to compute the performance of the missile. The missile geometry was modeled using the interface MissileLab. A series of simulations for different flight operating conditions was carried out. The primary quantities compared were the axial force coefficient, C_A and the skin friction coefficient, C_f . This Thesis describes the results obtained along with the geometry changes that became necessary to obtain reasonable agreement.

THIS PAGE INTENTIONALLY LEFT BLANK

TABLE OF CONTENTS

I.	INTRODUCTION.....	1
A.	DESCRIPTION OF WORK.....	1
B.	MISSILE PREDICTION EMPIRICAL SOFTWARE CODE	2
C.	OUTPUT ANALYSIS.....	3
D.	MISSILE PERFORMANCE	3
E.	IMPORTANCE OF C_A AND C_F ANALYSIS.....	4
1.	C_A Analysis	4
2.	C_F Analysis	6
3.	Other Force Components	7
II.	METHOD OF APPROACH.....	9
A.	DATA GIVEN	9
1.	MSIC Data Source	10
a.	Wind Tunnel Testing	10
b.	Simulink	12
B.	RESEARCH METHODOLOGY	13
1.	Geometry Coding.....	13
a.	Nose Geometry	13
b.	Fin Geometry.....	14
c.	Body Geometry	14
d.	Surface Roughness	14
2.	Operating Conditions	15
a.	Boundary Layer Conditions	15
b.	Fins Deflections	15
c.	Angle of Attack and Altitude	16
d.	Base Drag	16
III.	RESULTS	17
A.	SIMULATION CONDITIONS.....	17
B.	COMPONENTS INVOLVED IN AXIAL FORCE COEFFICIENT	19
C.	COEFFICIENT OF SKIN FRICTION	20
1.	Effects of Power on Coefficient of Skin Friction.....	20
2.	Effects of Surface Roughness on Coefficient of Skin Friction	21
3.	Effects of Mach Number on Coefficient of Skin Friction.....	23
4.	Effects of α on C_f	23
D.	AXIAL FORCE COEFFICIENT	23
1.	Effects of Power on Axial Force Coefficient.....	23
2.	Effects of Surface Roughness on Axial Force Coefficient	24
3.	Effects of Mach Number on Axial Force Coefficient.....	25
4.	Effects of Angle of Attack on Axial Force Coefficient.....	25
5.	Effects of Altitude on Axial Force Coefficient.....	26
E.	DATA COMPARISON WITH MSIC DATA	27
1.	Skin Friction Coefficient Comparison with MSIC Data	27

2.	Axial Force Coefficient Comparison with MSIC Data.....	28
IV.	CONCLUDING REMARKS	31
A.	LIMITATIONS	31
B.	FUTURE WORK	32
	LIST OF REFERENCES	33
	INITIAL DISTRIBUTION LIST	35

LIST OF FIGURES

Figure 1	Kill Envelope of Various Generations of the S-75 System [From 6]	3
Figure 2	Component Build-up Model [From 1]	5
Figure 3	Variation due to Mach Number of Drag Components [From 1]	6
Figure 4	C_f vs. Reynolds Number [From 1]	7
Figure 5	Missile Dimension Provided by MSIC	10
Figure 6	C_f vs. Reynolds Number [From 2]	12
Figure 7	Coded 3-D Sketch of Missile with Booster Attached from MissileLab	13
Figure 8	Coded 3-D Sketch of Missile After Booster Separation	14
Figure 9	C_A Components vs. Mach Number (Power Off, Turbulent, Roughness 0.001016, $\alpha = 0$ deg, Alt. = 0 m)	19
Figure 10	C_A Components vs. Mach Number (Power On, Turbulent, Roughness 0.001016, $\alpha = 0$ deg, Alt. = 0 m)	20
Figure 11	C_f vs. Mach Number (Power Off, Turbulent, Roughness 0.001016, 0 deg α)	21
Figure 12	C_f vs. Mach Number (Power On, Turbulent, Roughness 0.001016, 0 deg α)	21
Figure 13	C_f vs. Altitude (Power Off, Turbulent, Roughness 0.001016, 0 deg α)	22
Figure 14	C_f vs. Altitude (Power Off, Turbulent, Roughness 0, 0 deg α)	22
Figure 15	Comparison of Altitude and α Using C_f vs. Mach Number (Power Off, Turbulent, Roughness 0.001016)	23
Figure 16	Comparison of Altitude and α Using C_A vs. Mach Number (Power Off, Turbulent, Roughness 0.001016)	24
Figure 17	Comparison of Altitude and α Using C_A vs. Mach Number (Power On, Turbulent, Roughness 0.001016)	24
Figure 18	Comparison of Altitude and α Using C_A vs. Mach (Power Off, Turbulent, Roughness 0)	25
Figure 19	Comparison of α Using C_A vs. Mach Number (Power Off, Turbulent, Roughness 0, 0m)	26
Figure 20	Comparison of Altitude Using C_A vs. Mach Number (Power Off, Turbulent, Roughness 0)	26
Figure 21	C_f vs. Mach Number (Power Off, Turbulent, Roughness 0.001016, 0 deg α)	27
Figure 22	C_A vs. Mach Number (Power On, Turbulent, Roughness 0.001016, 0m, 0 deg α)	28
Figure 23	C_A vs. Mach Number (Power Off, Turbulent, Roughness 0.001016, 0m, 0 deg α)	29

THIS PAGE INTENTIONALLY LEFT BLANK

LIST OF TABLES

Table 1.	Flow Conditions for C_f Analysis.....	18
Table 2.	Flow Conditions for C_A Analysis	18

THIS PAGE INTENTIONALLY LEFT BLANK

ACKNOWLEDGMENTS

I would like to thank Professor M.S. Chandrasekhara for his continuous guidance. He has been a source of inspiration. Also, I would like to give special thanks to LCDR. Robert DeWitt, MSIC, for sponsoring and supporting this project, providing the wind tunnel and simulated performance data, and for following up steadily during the course of this work.

I would also like to give special thanks to Dr. William Blake of USAF and Mr. Lamar Auman, U.S. Army AMRDEC for permitting the use of Missile DATCOM (97) code and the U.S. Army MissileLab code. This made my task significantly easier.

I would like to express my gratitude to my wife, Clarice Chew and daughter Carlin Teo, who have supported me throughout my time in NPS. Their unwavering support and encouragement have made my Thesis process enjoyable.

NOMENCLATURE

C_A	=	Axial force coefficient
C_{Ab}	=	C_A due to base pressure
C_{Af}	=	C_A due to skin friction
C_{ALE}	=	Leading edge C_A
C_{A0}	=	C_A at zero normal force
C_{Ap}	=	C_A due to pressure
C_{ATE}	=	Trailing edge C_A
C_{Aw}	=	C_A due to wave drag
C_{Awn}	=	C_A due to nose
C_{Awa}	=	C_{Aw} due to after body
C_D	=	Coefficient of drag
C_{D0}	=	C_D at zero lift
C_f	=	Coefficient of skin friction
C_L	=	Coefficient of lift
C_N	=	Coefficient of normal force
C_p	=	Coefficient of pressure
Re	=	Reynolds number
α	=	Angle Alpha; Angle of Attack

I. INTRODUCTION

A. DESCRIPTION OF WORK

Aerodynamic predictions, using various prediction tools, have been practiced for many years. Comparisons and validations are usually made between computations, simulations, and wind tunnel test data in an attempt to predict actual flight performance. In this Thesis, a combination of experimental wind tunnel test data and simulations data became available for use to compare with that predicted by codes. This was an attempt to investigate the model geometry and flight conditions that will provide the aerodynamic properties matching the given data. When fully implemented and validated, the technique becomes another tool in the hands of an analyst to assess the performance of missile.

The missile system of particular interest to the sponsor was the SA-2 like configuration. Its flight characteristics were experimentally determined and subsequently also modeled. This combined data set for the missile system was provided by Missile and Space Intelligence Center (MSIC). Such data, however, tends to be incomplete due to limitations of testing some of which include altitude simulation, scale effects and free stream turbulence effects. Thus, it is imperative that the performance prediction code used be capable of allowing these factors to be included in the modeling to generate a resultant data base that can be used for a comprehensive range of flight conditions. Therefore, to validate and analyze the missile system, a methodology was developed to build up the missile model accurately using the US Army AMRDEC package, described as MissileLab [5]. It automatically generates the input files for the USAF missile performance evaluation code Missile Datcom (97) [4]. The design was put through several simulations. This involved studies at many different flow conditions, such as:

- Mach numbers
- Altitudes
- Angles of Attack
- Missile surface geometry conditions
- Boundary layer conditions

Results from such an extensive research analysis were analyzed and refined through changes in missile configurations or test conditions. These results were then compared to the data provided and comments and recommendations were made.

B. MISSILE PREDICTION EMPIRICAL SOFTWARE CODE

Although many prediction codes are available in the market, it is the sponsor's requirement to produce as many aerodynamic performance coefficients as possible that led to the use of Missile Datcom (97) [3]. Studies have been conducted to validate the results produced by Missile Datcom (97) and empirical data [3]. Under certain condition, results have shown [3] that prediction of axial force by Missile Datcom (97) falls within 11.69% accuracy. A similar and comparable performance prediction code, namely AP05, is available but it predicts fewer performance coefficients. It is more suitable for 2D modeling; whereas Missile Datcom (97) can be used for 3D aerodynamic prediction.

Missile Datcom (97) has many key features [3] which make it an attractive aerodynamic prediction tool. It possesses a trimmed flight function and is able to use experimental data to model a particular configuration. Missile Datcom (97) has the capability of modeling standard airfoil design and user defined airfoils. It also allows air breathing propulsion systems to be analyzed. However, it lacks plotting functions as well as geometry sketch functions, requiring the user to have a strong understanding on FORTRAN programming and the need for a post-processing tool. Although the output files for TECPLOT can be generated, the unavailability of this graphics package at NPS implied use of other methods. In this Thesis, post processing is done using Excel to present the results.

Interface with Missile Datcom (97) is through a Windows-based software known as MissileLab. MissileLab allows users with minimum knowledge of FORTRAN programming to utilize the aerodynamic prediction capability of Missile Datcom (97). One of the main features of MissileLab is the capability to produce 3D sketches of any parts of a missile configuration as it is being built, thereby eliminating user input errors.

C. OUTPUT ANALYSIS

From the data provided by MSIC and the time frame of the research available, two parameters of significant importance were analyzed in this Thesis. These were: axial force coefficient C_A for the body and fins and, also, C_A due to skin friction for the body only. Both these parameters provide insights into the performance of the missile as discussed below.

D. MISSILE PERFORMANCE

The SA-2 class missile in this Thesis operates in a wide range of conditions. The missile has a 2-stage propulsion system, with the booster detaching itself 3 to 5 seconds after launch. The main engine then provides the thrust for another 25 seconds before burning out [6]. By then, the missile would have reached Mach 3.

With its first employment in 1957 and its first successful publicized engagement of the U2 Reconnaissance aircraft in 1960 piloted by Francis Gary Powers [6], it has since been widely used in many air defense systems. The operating altitude of the U2 is 27,000m [6]. The missile is therefore required to operate over a wide regime of altitudes, accelerating through subsonic to supersonic and high Angle of Attacks (α) due to its maneuvering. The kill envelope is shown in Figure 7.



Figure 1 Kill Envelope of Various Generations of the S-75 System [From 6]

E. IMPORTANCE OF C_A AND C_F ANALYSIS

The standard coefficients such as various forces (axial, normal and side) and of the various moments are the quantities of interest. However, the wind tunnel test data placed notable emphasis on the axial force skin friction coefficient, with and without engine power. Thus, the comparisons to be made will focus on these two quantities. It is noted here that other quantities were also computed and would be discussed as well. The axial force is a critical quantity in the design of a missile and primarily determines the range and the maneuverability of the missile. In addition, the drag of a missile is a strong function of the flight Mach number. Different flow related mechanisms come into play at different speed regimes, as has been described in detail in [1]. As such, the aerodynamic prediction code must be capable of computing it by switching to the appropriate method of the computation based on the speed regime without user interference. Likewise, the skin friction also has to be computed based on the flow conditions at the wall.

Even though all these details are considered, it will still not be possible to properly quantify these for the actual vehicle owing to the scale effects even in modeling. This is particularly true for small protuberances and appendage that a full-scale missile carries and the inclusion of their effects on the potential flow pressure distribution at the various speed ranges and on each other.

1. C_A Analysis

It is well known that more than 50% of drag is body induced and thus, drag will be the primary focus in this Thesis through C_A analysis in the predictions of the performance of the given missile system. The study of C_A will allow predictions in the range of the missile, its speed, size of propulsion system, and its carriage effect on airborne systems. The overall C_A of a missile body is further broken down into C_{Af} (C_A due to skin friction) and C_{Ap} (C_A due to pressure). Thus,

$$C_{Ao} = C_{Af} + C_{Ap}$$

Predictions from C_A and C_N will then allow us to generate C_L and C_D of the missile using the following equations:

$$C_D = C_A \cos \alpha + C_N \sin \alpha$$

$$C_L = C_N \cos \alpha - C_A \sin \alpha$$

The general components making up the missile drag are shown in Figure 2. Drag prediction is done using a component buildup method by adding the individual drag of each component [1]. Missile Datcom (97) allows each component's drag coefficient to be analyzed.

As the missile operates through a wide range of Mach numbers, the drag components will vary significantly, as shown in Figure 3. At subsonic speeds, skin friction dominates while at higher Mach numbers, wave drag will dominate [1].

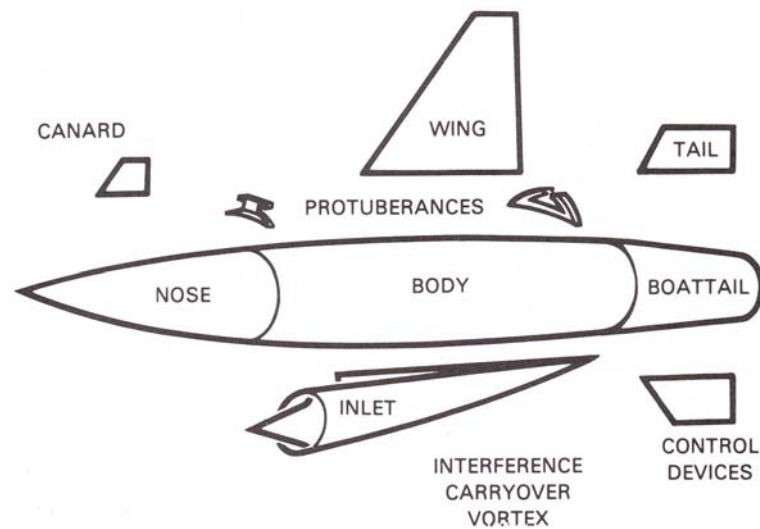


Figure 2 Component Build-up Model [From 1]

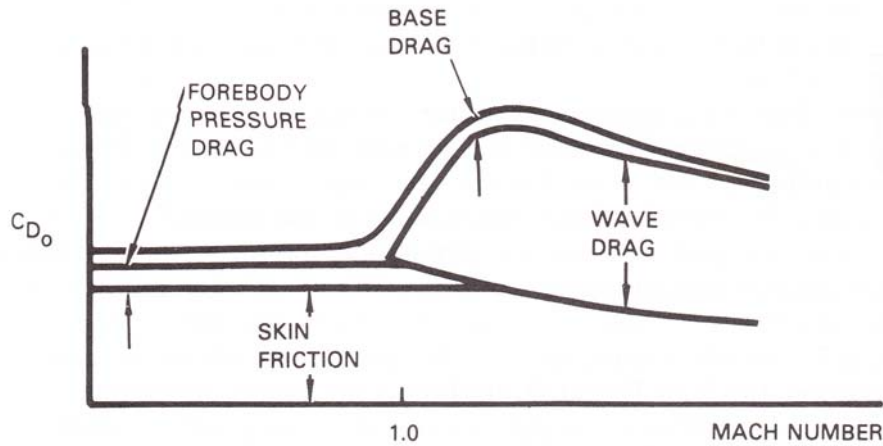


Figure 3 Variation due to Mach Number of Drag Components [From 1]

2. C_f Analysis

A boundary layer exists between the body of the missile and the freestream. The shear force due to fluid viscosity at the wall is the source of the skin friction drag. The amount of skin friction drag depends not only on whether the layer is laminar or turbulent and can vary as much as 10 times [1], but also on whether a laminar separation bubble forms at different altitudes and flow Reynolds numbers. In fact, multiple regions of local separation are also possible in missile flow due to many vane sets and differently deflected flaps. A turbulent flow condition generally results in higher C_f values; compared to a laminar flow condition. It is also well known that C_f strongly depends on Reynolds number as shown below [2]:

$$Re = \frac{\rho_{\infty} V_{\infty} d}{\mu_{\infty}}$$

As Re increases, C_f decreases. And since the missile in question has an operating altitude from 0 to 30000m, it is crucial that thorough understanding be made of its operating conditions because its unit Reynolds number can change by three orders of magnitude from 10^5 to 10^8 .

Typical Reynolds number for the three different flow conditions: Laminar, Transitional and Turbulent is shown in Figure 4.

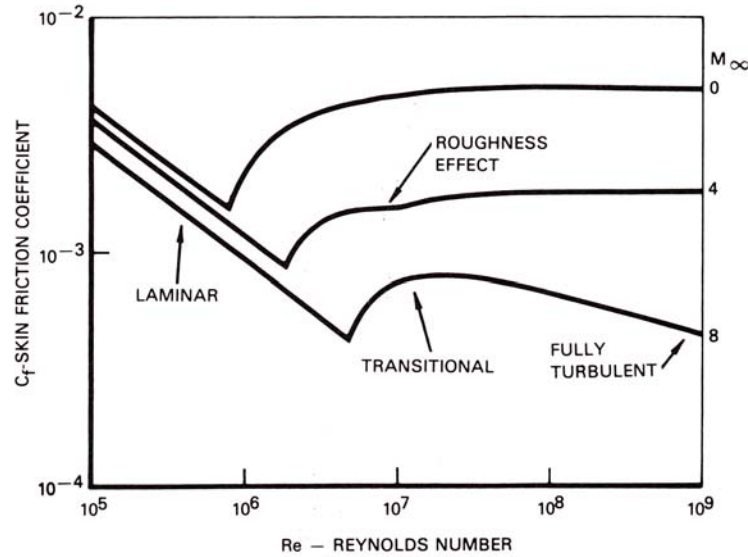


Figure 4 C_f vs. Reynolds Number [From 1]

3. Other Force Components

In addition, the general flow over a missile is very complicated. The strong vortical flow at angles of attack which develops over a body of revolution that comprises the missile also affects the local flow and its separation. This can be especially significant at large pitch and roll angles. The asymmetric formation of these structures and their interactions could lead to very large and unexpected side forces that are difficult to predict. Furthermore, these lead to unsteady forces that affect the maneuver characteristics of the missile. Thus, even though much emphasis is placed on analyzing the axial force and skin friction behavior, the other aspects are also briefly considered.

THIS PAGE INTENTIONALLY LEFT BLANK

II. METHOD OF APPROACH

A. DATA GIVEN

A limited aerodynamic data set was provided by MSIC for comparison and use in this study. As already stated, this is a combination of experiments and simulation. Thus, the data set represents a sparse matrix of flow conditions and to a part of the much larger aerodynamic flight regime of the missile. Furthermore, since the SA-2 type missile is an incoming missile, it is difficult to establish the full performance details easily. In the data set provided, the skin friction values are given only for $0 \text{ deg } \alpha$.

MSIC also provided the geometry of the missile and is at best estimated from a scaled diagram with minimum dimensions. Most parts of the geometry are estimated through scaling and knowledge based on high speed missile systems. These estimations include airfoil geometry (cross section), nose geometry, center of gravity, and pivoting points for the wing control surfaces.

that can be achieved in wind tunnel testing is about $10^5 - 10^6$. On the other hand, the missile experiences at least an order of magnitude higher unit Reynolds number over the different altitudes that it flies in. Thus, unless the boundary layer is tripped artificially to reproduce the effects of the higher flight Reynolds number, the laboratory data includes the effect of natural transition in addition to the presence of natural laminar flow over some of the body length. In order to induce transitional and turbulent flow over the object, trips were employed. However, utilization of trips to create the required flow condition is indeed an art and to accomplish it consistently to obtain different Reynolds numbers is difficult.

Another well known limitation is the scale effect created due to the necessarily smaller scale of the laboratory scale model. A full scale wind tunnel testing of the model will not be practical. With a scaled model, the forces acting on the test object will be reduced proportionately while the coefficients remain the same. This reduction will increase measurement difficulties and reduce the accuracy of the measurements. For incompressible laminar flow over a flat plate the integrated skin friction coefficient [2] is:

$$C_f = \frac{1.328}{\text{Re}_c^{1/2}}$$

And for incompressible turbulent flow [2]:

$$C_f = \frac{0.074}{\text{Re}_c^{1/5}}$$

Thus, the laminar and turbulent skin friction coefficients vary as $\text{Re}^{-1/2}$ and $\text{Re}^{-1/5}$ respectively. As Reynolds number depends on the overall length 'c' over which the fluid is flowing, testing on smaller scale models tends to reduce the overall skin friction values when compared to that are encountered by the full scale missile. The relationship between C_f values and Reynolds number is shown in Figure 6.

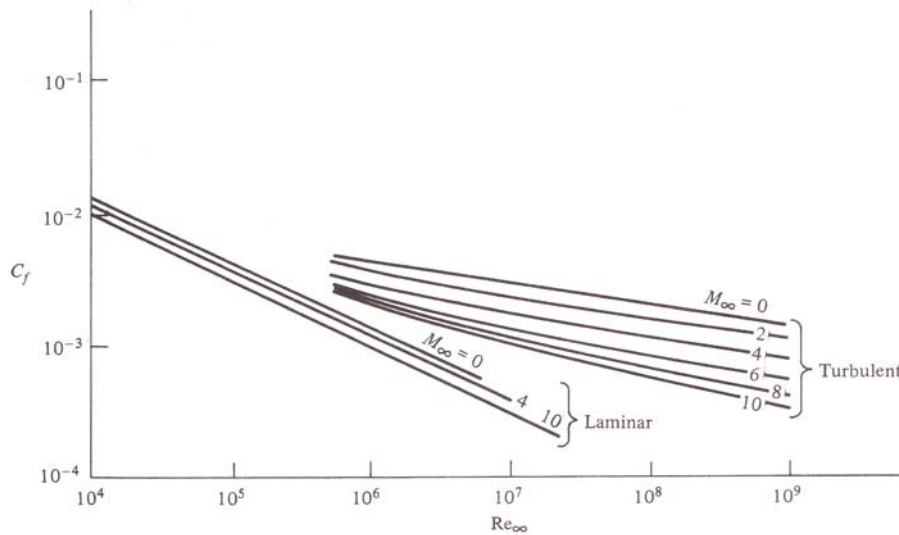


Figure 6 C_f vs. Reynolds Number [From 2]

Determination of these quantities over the full range of flight Mach numbers from subsonic through to hypersonic in the laboratory is a significant challenge. There is no one wind tunnel that can cover this wide range of flow conditions. The wind tunnel size tends to decrease as the Mach number increases. The test times also decrease. To minimize wind tunnel blockage effects, the models become even smaller at the higher Mach numbers. Thus, the uncertainty associated with the test data on some of the quantities of interest here increases. This is one of the reasons for extrapolating the wind tunnel test data to generate Simulink data for the higher flight conditions.

b. Simulink

A portion of the data given is supplemented by results generated from MATLAB/ Simulink modeling. This model is, however, developed from mathematical flight mechanics models, measured airframe properties and generated aerodynamic performance quantities. Thus, it lacks the fidelity and prediction capabilities of the 3-dimensional 6 DOF aerodynamic prediction software. A prominent limitation, for example, was the state of boundary layer on the missile -- whether it was natural, transitional, or fully turbulent.

B. RESEARCH METHODOLOGY

1. Geometry Coding

Coding of the geometry is done through MissileLab. The Windows User Interface in MissileLab enables users to check the geometry at every input stage. This includes 3-dimensional sketches of every component. This eliminates the need for tedious FORTRAN programming. To reduce design errors, MissileLab includes a self-check process to ensure that all geometries are consistent. A 3-dimensional sketch output from MissileLab is shown in Figure 7. This view is available throughout the geometry input stage allowing the user to make changes as needed.

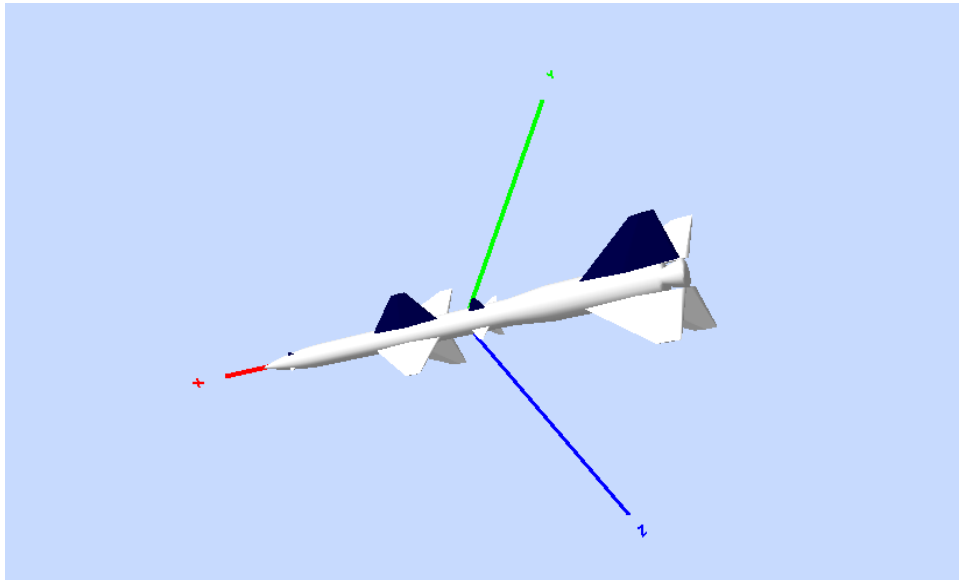


Figure 7 Coded 3-D Sketch of Missile with Booster Attached from MissileLab

a. Nose Geometry

A tangential ogive nose has been selected based on the scaled drawing provided by MSIC. This ensures that there is no discontinuity in the curvature at the nose-body junction.

b. Fin Geometry

Fin geometries are measured by hand to the best of the author's ability. The thickness of the fins and geometry of the airfoil have been selected based on knowledge of supersonic missiles. The geometry of the airfoil is an elliptical shape.

Due to the lack of detailed technical drawings, the pivot point for controllable fins is assumed to be in the middle of the cord length.

c. Body Geometry

The data given for the body was with the booster attached. MSIC's interest, however, is in the missile body aerodynamics after the booster separation phase. This occurs 3 to 5 seconds after launch. The MissileLab output for the missile after booster separation is shown in Figure 8

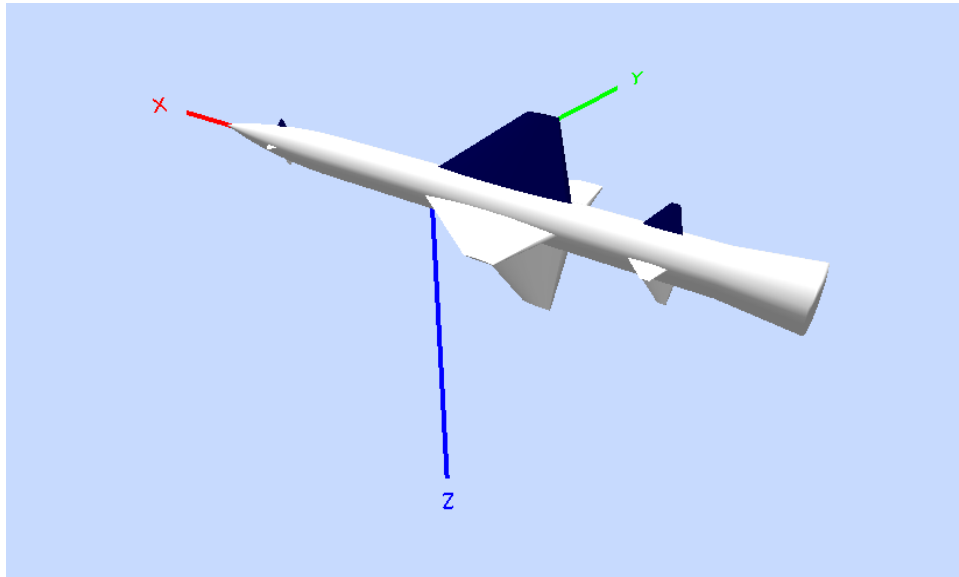


Figure 8 Coded 3-D Sketch of Missile After Booster Separation

d. Surface Roughness

As surface roughness was not recorded in the data given by MSIC, an iterative process was adopted in an attempt to map the data provided. For C_A mapping, even for a smooth surface (roughness = 0,) computed C_A values from MissileLab yielded

readings well above those from MSIC tests. In the C_f mapping, using a surface roughness of 0.001016 produced results that were very close to the data provided. Therefore, this surface roughness has been selected. It is equivalent to a relatively smooth surface on which the paint is carefully applied. More discussions on the comparison will be carried out in later sections.

2. Operating Conditions

In general, the SA-2 type missile can operate over a wide range of flow conditions from $M = 0.8$ to $M = 2.5$. However, the modern missiles may be expected to fly at even a higher speed range and also perform maneuvers that are quite dramatic and uncommon. Due to lack of specific data on the operating conditions of the missile, several permutations of conditions were arbitrarily selected for predicting the missile performance.

a. Boundary Layer Conditions

The state of the boundary layers is a significant parameter in the aerodynamic coefficients of interest. The large change in Reynolds number with the significant change in the altitude experienced by the missile means that both natural and fully turbulent boundary conditions have to be modeled. In addition, a combination of the two as also the possible formation of a laminar separation bubble will need to be considered at very high altitudes due to the large kinematic viscosity of air that can drop the Reynolds number to sufficiently low values where the effects of the bubble can begin to alter the skin friction values and also, C_A significant. This was not pursued, however.

b. Fins Deflections

A trimmed flight condition has been modeled with no fin deflections.

c. Angle of Attack and Altitude

Twelve angles of attack, α values were used in the simulations starting from 0 deg α to 24 deg α in increments of 2 deg. Altitudes selected were 0m, 5000m, 10000m, 20000m, and 30000m.

d. Base Drag

With base drag forming as much as 50% of the total missile, data was obtained with Base Drag (power off) and without Base Drag (power on) for comparison. Moreover, after booster separation, the missile will continue to receive thrust from its second stage propulsion for another 20 seconds before cruising without power in the terminal stage. This necessitates the need to obtain data for both power on and power off. Based on MSIC recommendations, this Thesis' work will focus on the power off condition. This is because of the missile flies under these conditions during the later stage of the cruise profile and, most importantly, in the terminal phase.

III. RESULTS

A. SIMULATION CONDITIONS

Part of the effort was aimed at generating the missile aerodynamic performance characteristics at conditions that envelope the flow conditions for which MSIC has supplied either the test data or the simulation data. It is also hoped that after establishing confidence in the computations by validating against the measured data, the characteristics for intermediate flow conditions can also be provided through this effort. The conditions chosen are shown in Table 1.

Power	Boundary Layer Conditions	Surface Roughness	Plots	Varying (Altitude: m)	Fixed (α : deg)
Off	Natural	Smooth	C_f vs. Altitude	Mach Number (1.2, 3, 4.5)	0
			C_f vs. Mach Number	Altitude (5000, 30000)	0
			C_f vs. Altitude	Mach Number (1.2, 3, 4.5)	12
			C_f vs. Mach Number	Altitude (5000, 30000)	12
	Rough		C_f vs. Altitude	Mach Number (1.2, 3, 4.5)	0
			C_f vs. Mach Number	Altitude (5000, 30000)	0
			C_f vs. Altitude	Mach Number (1.2, 3, 4.5)	12
			C_f vs. Mach Number	Altitude (5000, 30000)	12
On	Natural	Smooth	C_f vs. Altitude	Mach Number (1.2, 3, 4.5)	0
			C_f vs. Mach Number	Altitude (5000, 30000)	0
			C_f vs. Altitude	Mach Number (1.2, 3, 4.5)	12
			C_f vs. Mach Number	Altitude (5000, 30000)	12
	Rough		C_f vs. Altitude	Mach Number (1.2, 3, 4.5)	0
			C_f vs. Mach Number	Altitude (5000, 30000)	0
			C_f vs. Altitude	Mach Number (1.2, 3, 4.5)	12
			C_f vs. Mach Number	Altitude (5000, 30000)	12
Off	Turbulent	Smooth	C_f vs. Altitude	Mach Number (1.2, 3, 4.5)	0
			C_f vs. Mach Number	Altitude (5000, 30000)	0
			C_f vs. Altitude	Mach Number (1.2, 3, 4.5)	12
			C_f vs. Mach Number	Altitude (5000, 30000)	12
	Rough		C_f vs. Altitude	Mach Number (1.2, 3, 4.5)	0
			C_f vs. Mach Number	Altitude (5000, 30000)	0
			C_f vs. Altitude	Mach Number (1.2, 3, 4.5)	12
			C_f vs. Mach Number	Altitude (5000, 30000)	12
On	Turbulent	Smooth	C_f vs. Altitude	Mach Number (1.2, 3, 4.5)	0
			C_f vs. Mach Number	Altitude (5000, 30000)	0
			C_f vs. Altitude	Mach Number (1.2, 3, 4.5)	12

			C_f vs. Mach Number	Altitude (5000, 30000)	12
		Rough	C_f vs. Altitude	Mach Number (1.2, 3, 4.5)	0
			C_f vs. Mach Number	Altitude (5000, 30000)	0
			C_f vs. Altitude	Mach Number (1.2, 3, 4.5)	12
			C_f vs. Mach Number	Altitude (5000, 30000)	12

Table 1. Flow Conditions for C_f Analysis

Power	Boundary Layer Conditions	Surface Roughness	Plots	Varying (α : deg)	Fixed (m)
Off	Natural	Smooth	C_A vs. α	Mach Number (1.2, 3, 4.5)	0
			C_A vs. Mach Number	α (0, 12)	0
			C_A vs. α	Mach Number (1.2, 3, 4.5)	20000
			C_A vs. Mach Number	α (0, 12)	20000
		Rough	C_A vs. α	Mach Number (1.2, 3, 4.5)	0
			C_A vs. Mach Number	α (0, 12)	0
			C_A vs. α	Mach Number (1.2, 3, 4.5)	20000
			C_A vs. Mach Number	α (0, 12)	20000
On	Natural	Smooth	C_A vs. α	Mach Number (1.2, 3, 4.5)	0
			C_A vs. Mach Number	α (0, 12)	0
			C_A vs. α	Mach Number (1.2, 3, 4.5)	20000
			C_A vs. Mach Number	α (0, 12)	20000
		Rough	C_A vs. α	Mach Number (1.2, 3, 4.5)	0
			C_A vs. Mach Number	α (0, 12)	0
			C_A vs. α	Mach Number (1.2, 3, 4.5)	20000
			C_A vs. Mach Number	α (0, 12)	20000
Off	Turbulent	Smooth	C_A vs. α	Mach Number (1.2, 3, 4.5)	0
			C_A vs. Mach Number	α (0, 12)	0
			C_A vs. α	Mach Number (1.2, 3, 4.5)	20000
			C_A vs. Mach Number	α (0, 12)	20000
		Rough	C_A vs. α	Mach Number (1.2, 3, 4.5)	0
			C_A vs. Mach Number	α (0, 12)	0
			C_A vs. α	Mach Number (1.2, 3, 4.5)	20000
			C_A vs. Mach Number	α (0, 12)	20000
On	Turbulent	Smooth	C_A vs. α	Mach Number (1.2, 3, 4.5)	0
			C_A vs. Mach Number	α (0, 12)	0
			C_A vs. α	Mach Number (1.2, 3, 4.5)	20000
			C_A vs. Mach Number	α (0, 12)	20000
		Rough	C_A vs. α	Mach Number (1.2, 3, 4.5)	0
			C_A vs. Mach Number	α (0, 12)	0
			C_A vs. α	Mach Number (1.2, 3, 4.5)	20000
			C_A vs. Mach Number	α (0, 12)	20000

Table 2. Flow Conditions for C_A Analysis

B. COMPONENTS INVOLVED IN AXIAL FORCE COEFFICIENT

The total axial force component of a missile includes several components. Missile Datcom (97) calculates the axial force coefficient by including the various components of friction, pressure/wave, and base drag for the missile body as well as all the fins. In addition, the values arising from their interference are also calculated and output in a table. The contributions of each of these factors are shown in Figure 9 and Figure 10. It can be seen that base drag is the largest component and it contributes almost 50% to the overall missile axial force coefficient C_A . There is also a significant change in C_A with Mach number, which will be discussed in later sections.

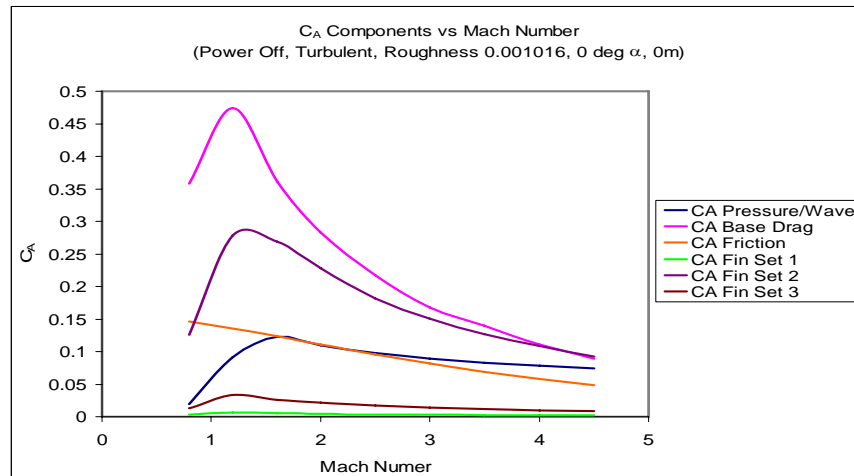


Figure 9 C_A Components vs. Mach Number (Power Off, Turbulent, Roughness 0.001016, $\alpha = 0$ deg, Alt. = 0 m)

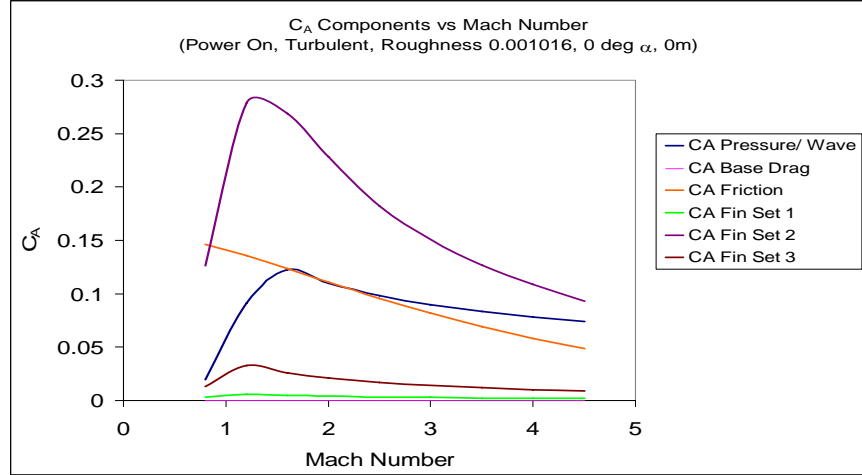


Figure 10 C_A Components vs. Mach Number (Power On, Turbulent, Roughness 0.001016, $\alpha = 0$ deg, Alt. = 0 m)

C. COEFFICIENT OF SKIN FRICTION

1. Effects of Power on Coefficient of Skin Friction

The effects of power on a missile showed no change to the skin friction coefficient as seen in both Figure 11 and Figure 12 where C_f is plotted for altitudes of 5000 m and 30,000 m. for the power off conditions. The skin friction values decrease monotonically with Mach number, perhaps due to increasing Reynolds number over the body length. The nearly parallel curves lend support to this inference. The value at the higher altitude is higher possibly due to the increased viscosity (by nearly two orders) at the very large altitude of 30,000m for which this computation was carried out. However, turning the power 'On' or 'Off' did not significantly affect the base drag.

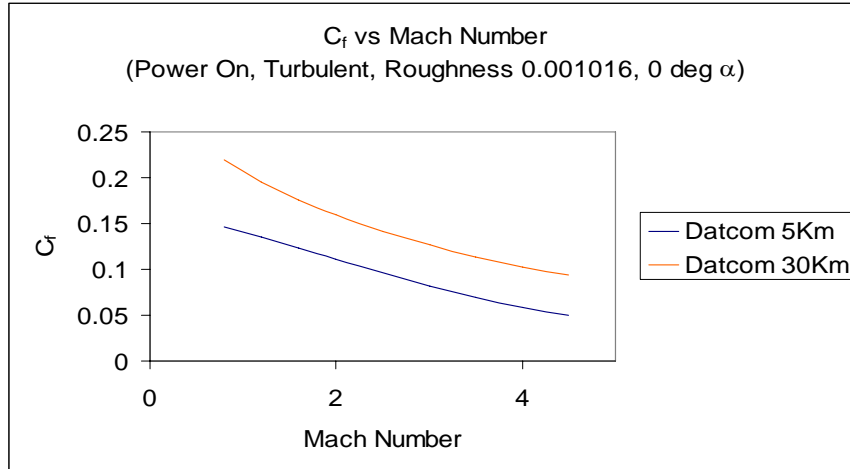


Figure 11 C_f vs. Mach Number (Power Off, Turbulent, Roughness 0.001016, 0 deg α)

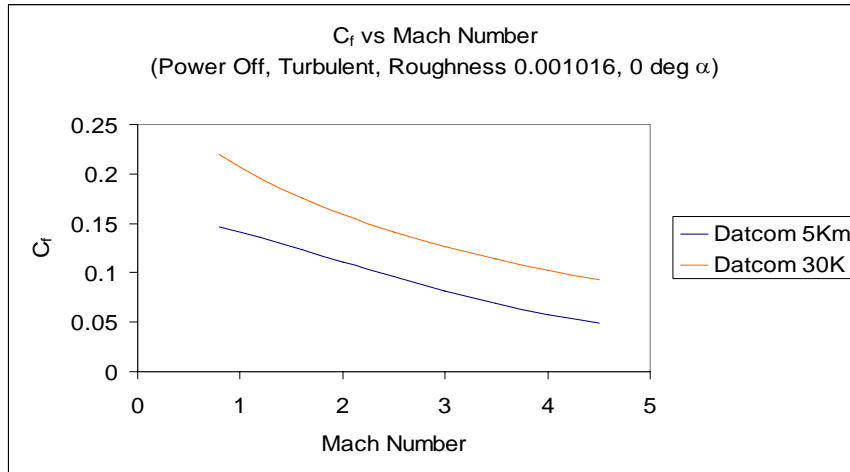


Figure 12 C_f vs. Mach Number (Power On, Turbulent, Roughness 0.001016, 0 deg α)

2. Effects of Surface Roughness on Coefficient of Skin Friction

Skin friction is largely affected by the state of the boundary layer forming on the missile surface. Surface roughness plays an important role in altering the boundary layer state and thus, in determining skin friction drag. Figure 13 and Figure 14 show plots with a surface roughness of zero compared to a surface roughness of 0.001016m. On a real missile, this roughness value represents a reasonably well painted surface. The plots from Missile Datcom showed significantly lower C_f values at lower altitude (20000m) for a smooth surface. Above 20000m, C_f was observed to be insensitive to surface roughness.

An analysis of the variation of the properties of air with altitude shows that up to 20000 m, the kinematic viscosity increase by an order, however between 20000 m and 30000 m, it raises by an order. Thus, at an altitude of 20000m and above, the Reynolds number can be as low as $3.0E+05$. This resulted in a thick laminar layer in which the roughness height was only a small fraction of the total boundary layer height, which caused the C_f to become insensitive to surface roughness. Another possibility is the formation of a long laminar bubble at low Reynolds number and thus having surface roughness insensitive C_f values due to local flow separation inside the bubble.

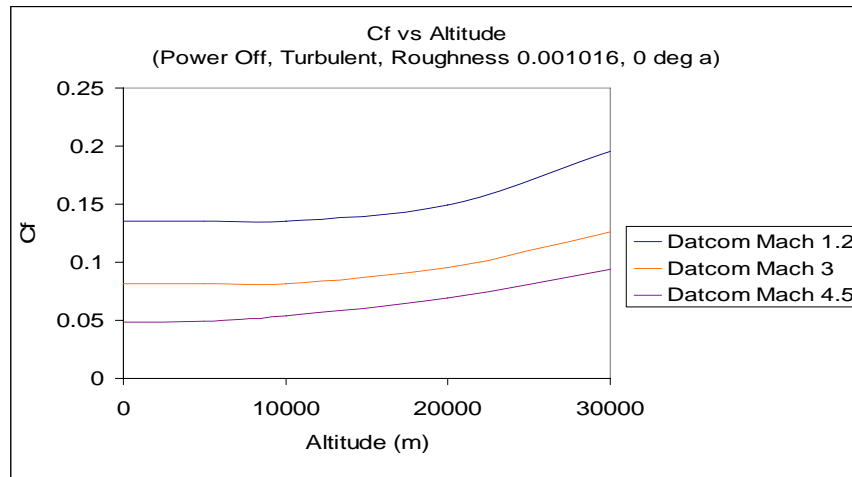


Figure 13 C_f vs. Altitude (Power Off, Turbulent, Roughness 0.001016, 0 deg α)

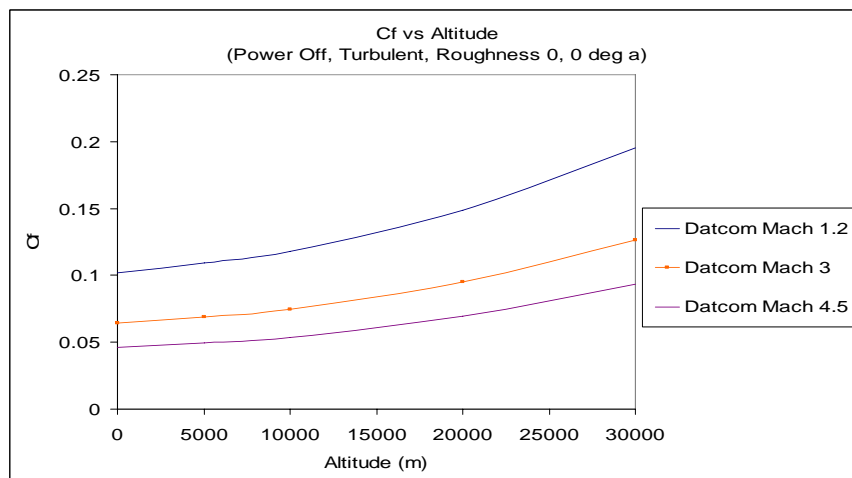


Figure 14 C_f vs. Altitude (Power Off, Turbulent, Roughness 0, 0 deg α)

3. Effects of Mach Number on Coefficient of Skin Friction

C_f values generally decrease with increasing Mach number as seen in Figure 13 and Figure 14. The lowest C_f values are observed for the highest Mach number of 4.5 for the missile. The insensitivity of C_f at M 4.5 is still being analyzed.

4. Effects of α on C_f

C_f values for different angles of attack are plotted in Figure 15. Increasing α reduces the C_f values, although not as drastically as increasing the Mach numbers. This can be seen in Figure 15. As the missile increases in α , separation of air begins which reduces the viscous effect and results in lower C_f values.

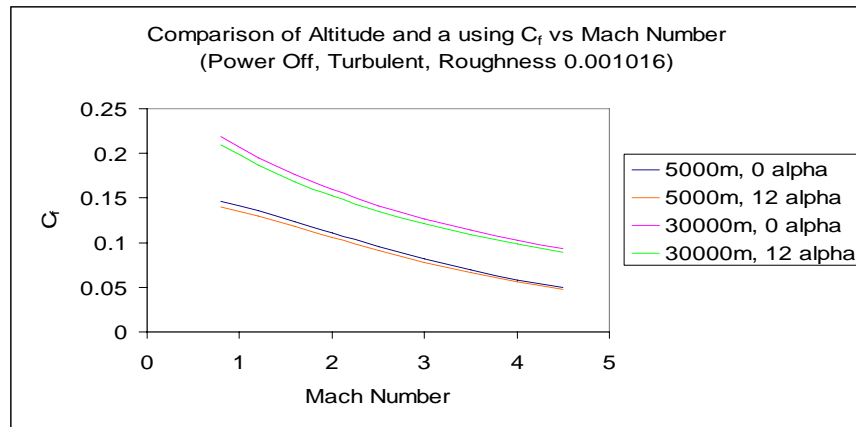


Figure 15 Comparison of Altitude and α Using C_f vs. Mach Number (Power Off, Turbulent, Roughness 0.001016)

D. AXIAL FORCE COEFFICIENT

1. Effects of Power on Axial Force Coefficient

Without power, the base drag of a missile can be as high as 50% of the total drag [1]. For the power off condition in Figure 16 the average C_A is about 1.0 and, in Figure 17 the average C_A is about 0.55. That is a significant increase of 45% in C_A with power off.

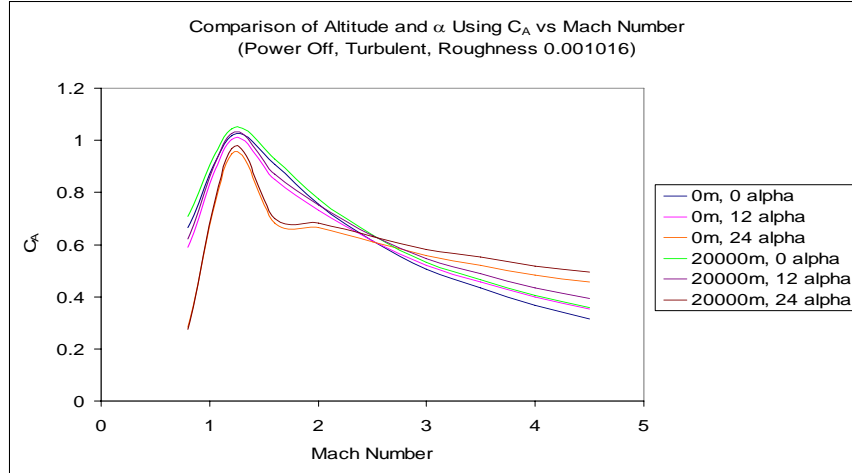


Figure 16 Comparison of Altitude and α Using C_A vs. Mach Number (Power Off, Turbulent, Roughness 0.001016)

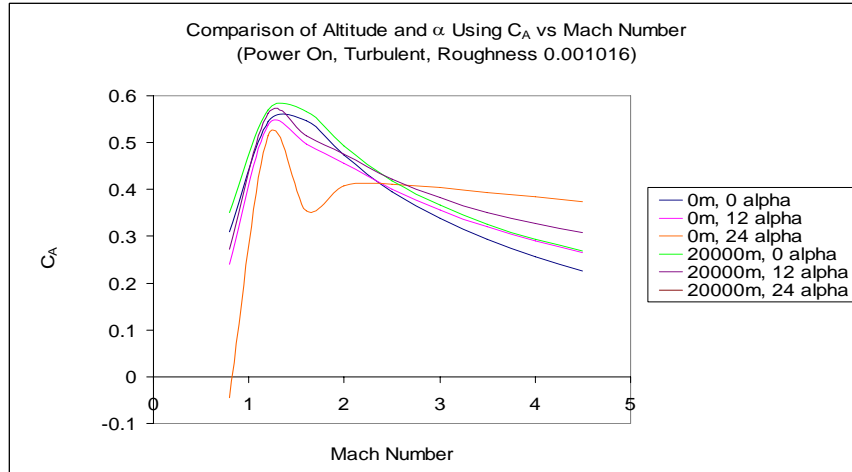


Figure 17 Comparison of Altitude and α Using C_A vs. Mach Number (Power On, Turbulent, Roughness 0.001016)

2. Effects of Surface Roughness on Axial Force Coefficient

At 0m, C_A reduces slightly with smooth surfaces, as shown in Figure 16 and Figure 18. This is an expected phenomenon as a smooth surface will have a reduced C_f resulting in overall C_A . However, in both plots, at an altitude of 20000m, C_A becomes relatively insensitive to surface roughness. The lower Reynolds number at high altitude ($3.0E+05$) causes C_f to vary little as discussed in Figure 6. Thus, the resulting C_A remains unaffected.

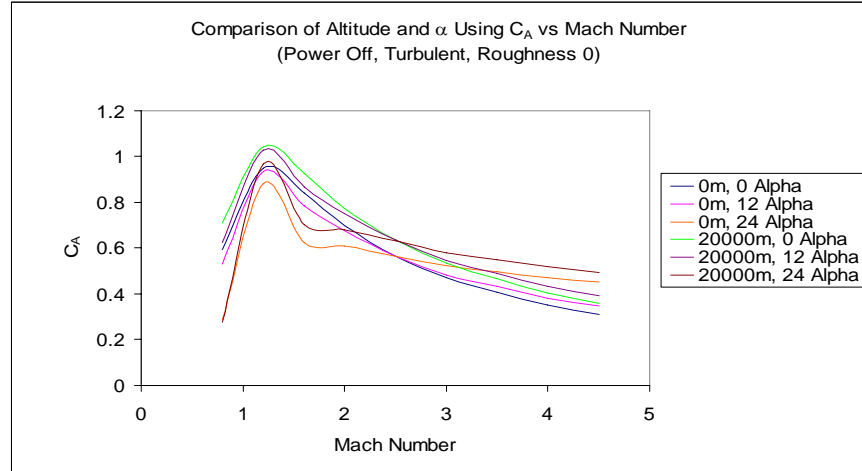


Figure 18 Comparison of Altitude and α Using C_A vs. Mach (Power Off, Turbulent, Roughness 0)

3. Effects of Mach Number on Axial Force Coefficient

Variations of Mach number have a very large change on the axial force, as can be seen in Figure 18. Most changes are observed through the transonic Mach number regime. At transonic speeds, shocks begin to form on the missile body. The shocks that form interact with the local boundary layer, shock oscillations also can be present and an abrupt increase in pressure drag occurs and thus also, in the C_A values. As the Mach number continues to increase, these shocks will move towards the nose and the tail and become detached from the missile body. The air on the missile body will now see a velocity slower than the free-stream velocity and, thus, result in lower C_A values.

4. Effects of Angle of Attack on Axial Force Coefficient

With Mach number less than 2.5, increasing the angle of attack results in lower C_A values as shown in Figure 19. This is due to flow separation from the surface of the missile body. The kink seen for the case of $\alpha = 24$ deg seems to indicate that this is a likely scenario. Above Mach 2.5, a crossover in C_A can be seen. This could be due to the possibility of asymmetric vortices being generated, which is typical of missile body at high angles of attack. These vortices will also induce side forces on the missile body, further affecting the resulting overall C_A .

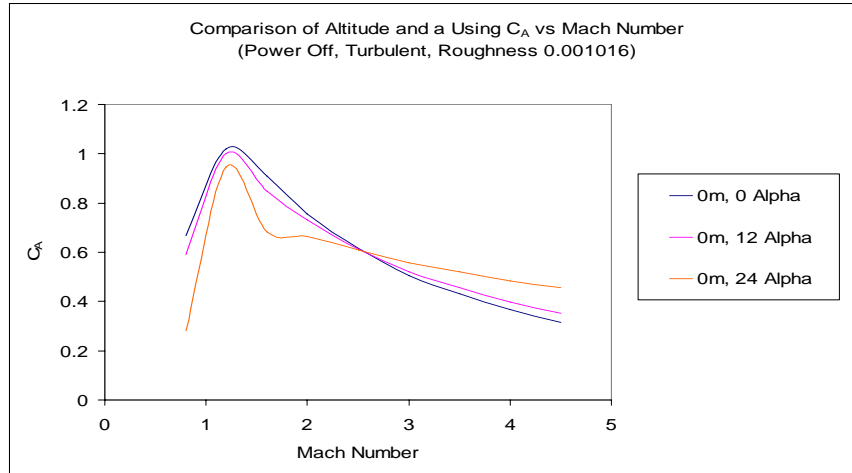


Figure 19 Comparison of α Using C_A vs. Mach Number (Power Off, Turbulent, Roughness 0, 0m)

5. Effects of Altitude on Axial Force Coefficient

As altitude increases, C_A increases as shown in Figure 20. As explained in Figure 12 and Figure 13 earlier, C_f value can increase with altitude as the Reynolds number becomes smaller. It should be noted here that C_f constitutes about 20-30% of the total axial force.

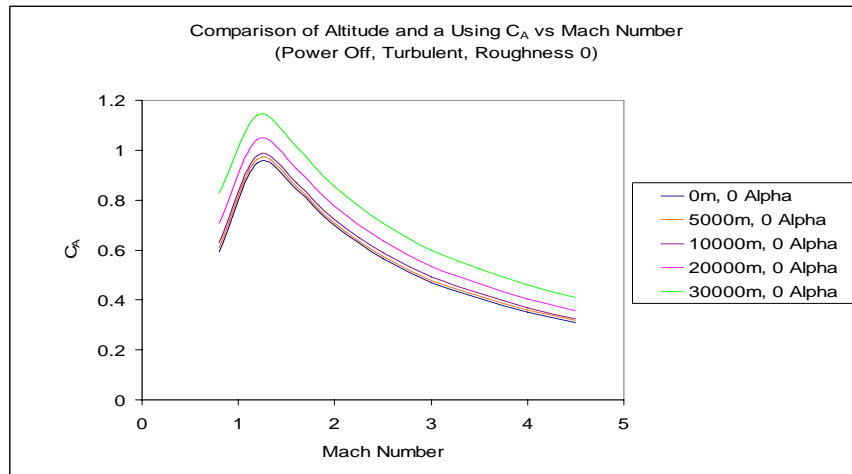


Figure 20 Comparison of Altitude Using C_A vs. Mach Number (Power Off, Turbulent, Roughness 0)

E. DATA COMPARISON WITH MSIC DATA

1. Skin Friction Coefficient Comparison with MSIC Data

The values for C_A due to friction are close to the data provided by MSIC by using a surface roughness of 0.001016 at an altitude of 5000m as shown in Figure 21. With similar surface roughness, however, the data does not match at an altitude of 30000m. At 30000m, the same roughness may correspond to a different relative roughness since the boundary layer is much thicker and the Reynolds number is much lower. Thus, obtaining a better match with the data will require experimenting with different surface roughness values. It is not clear whether the Simulink model included these effects. As mentioned earlier, wind tunnel testing typically gives lower Reynolds numbers compared to values obtained from actual airplane flight [2]. Studies have shown that low Reynolds number shows high-drag coefficients. MSIC data shows a trend of over-predicting the C_f values in Figure 21. This could be an indication of the low Reynolds number generally realized in wind tunnel testing. Disparity from Missile Datcom (97) result is more prominent at 30000m. At very high altitudes of 30000m, where the medium possess large deviations in properties from sea level, actual flight characteristics of the missile will prove difficult to replicate in wind tunnels.

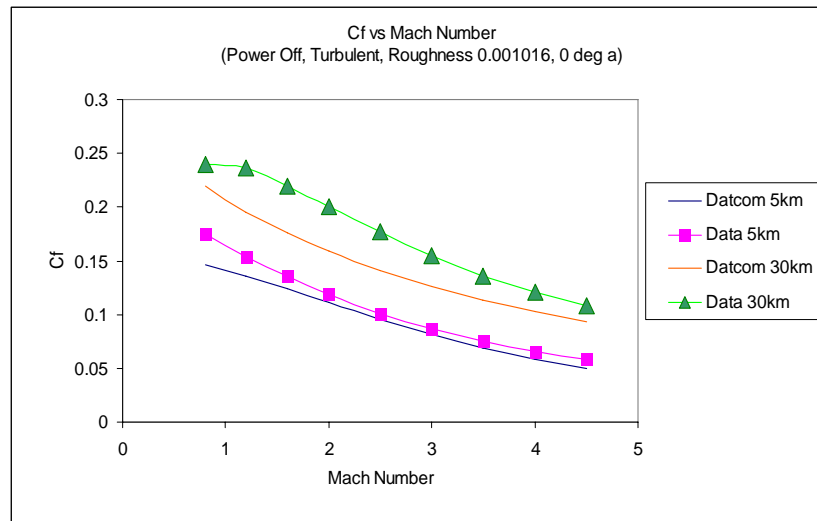


Figure 21 C_f vs. Mach Number (Power Off, Turbulent, Roughness 0.001016, 0 deg α)

2. Axial Force Coefficient Comparison with MSIC Data

Through clarification with MSIC, the C_A data provided consists of C_A due to pressure drag and C_A due to base drag. For power 'on' condition, a relatively close match from MissileLab can be achieved. Both data can be matched relatively closely at lower Mach numbers up to Mach 2.0 as shown in Figure 22. This could indicate the possibility of inaccuracies in the creation of flow conditions for high Mach numbers in wind tunnel environment.

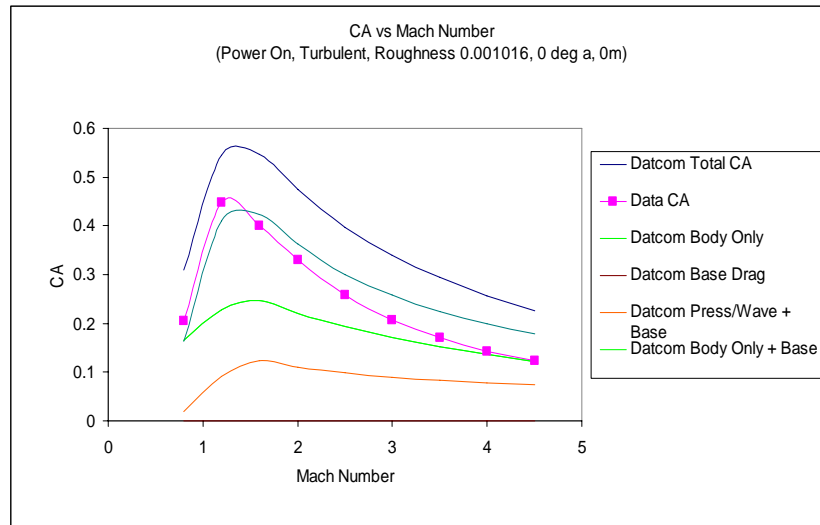


Figure 22 C_A vs. Mach Number (Power On, Turbulent, Roughness 0.001016, 0m, 0 deg α)

For the power 'off' condition, a relatively close match can be achieved by mapping the base drag from Missile Datcom output. The C_A values from MSIC, however, are notably lower and appear to capture only the base drag component.

With the assumption that MISC data captures only the base drag, results from Missile Datcom (97) show a relatively close match. Parameters affecting base drag include Reynolds number, Mach number, α , body fineness ratio, fin proximity, and the presence of a boat tail or flare [1]. But the contribution of Reynolds number, α , fineness ratio and fin proximity to base drag is small, and hence, the satisfactory match.

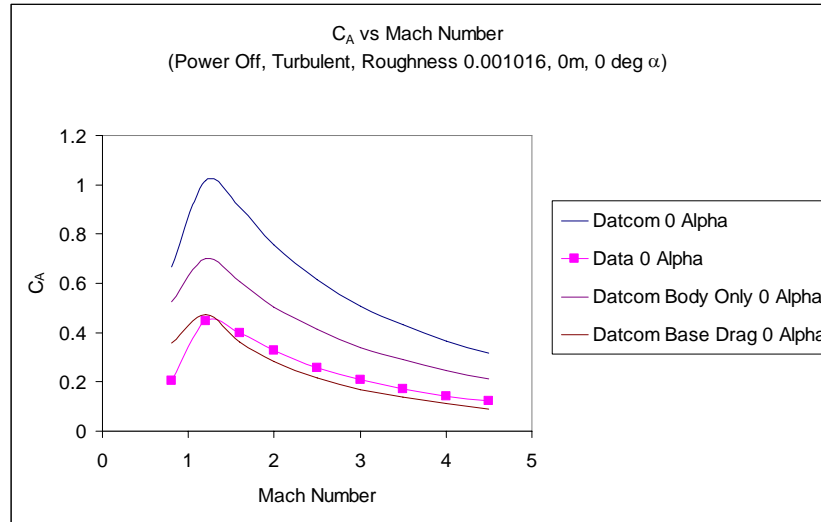


Figure 23 C_A vs. Mach Number (Power Off, Turbulent, Roughness 0.001016, 0m, 0 deg α)

In both cases, as C_A is a function of Mach number and Reynolds number, reproductions of the true operating conditions are crucial, and this is a challenge in wind tunnel testing and software modeling.

THIS PAGE INTENTIONALLY LEFT BLANK

IV. CONCLUDING REMARKS

A systematic study using DoD supplied empirical software packages was carried out to generate the aerodynamic performance coefficients of an SA-2 class missile. The results were compared against a data set provided by MSIC. The model geometry was generated using MissileLab and the computations were conducted using Missile Datcom (97). The study enveloped a large matrix of flow conditions. A reasonable match was obtained for C_f using a roughness of 0.000106m at sea-level conditions. At higher altitudes, a mismatch remained and this difference was explained as due to the effects of relative roughness that change steadily with altitude owing to the state of the boundary layer and its height changes concomitant with the Reynolds number changes with altitude. For C_A , a good match was obtained for the power 'on' condition up to about Mach 2.0. Additional work needs to be carried out for a higher degree of agreement.

A. LIMITATIONS

This study has some limitations, ranging from the use of a geometry that is derived from visual observations and also, from generating it from scaled figures. Data from a limited experimental test matrix was the basis for comparison of the computed and test results. The well known, inherent limitations of test data limit the range of comparisons that can be made. Factors such as free-stream turbulence, scaling effects and Reynolds number simulation affect the wind tunnel testing results which were not included in the studies.

Despite its capabilities, Missile Datcom also has some limitations which are reported in the literature. Future studies can overcome these by modeling the appropriate flow regimes for estimation of C_A suitably. Improvements have also been made in later versions of Missile Datcom through the investigation of fin normal force and center of pressure prediction [8].

With increasing computing powers, use of CFD to solve complex aerodynamic problems can provide more comparable results.

B. FUTURE WORK

One of the objectives for this Thesis was to set up an in-house capability for missile performance computation. Due to the limited amount of time available for this Thesis, operating conditions and analysis of the missile were restricted to a few values. Further iterations on the conditions can be made with added simulation runs performed on missile geometry changes, such as trimmed flights or varying the wings deflection.

LIST OF REFERENCES

- [1] Michael R. Mendenhall, Tactical Missile Aerodynamics: Prediction Methodology, Progress in Astronautics and Aeronautics, Volume 142, 1992, pp. 1-60.
- [2] John D. Anderson, Jr., Fundamentals of Aerodynamics, 2001, pp. 60-71.
- [3] Thomas J. Sooy and Rebecca Z. Schmidt, Aerodynamics Predictions, Comparisons and Validations Using Missile Datcom (97) and Aeroprediction 98 (AP98), AIAA 2004, 1246, 2004.
- [4] William B. Blake, Missile Datcom User's Manual - 1997 FORTRAN 90 Revision, AFRL-VA-WP-TR-1998-3009, 1998.
- [5] Lamar M. Auman, MissileLab User's Guide, AMR-SS-06-12, Feb 2006.
- [6] Steven Zaloga, Red Sam: The SA-2 Guideline Anti-Aircraft Missile (New Vanguard), 2007.
- [7] Amanda N. Horton and Melissa A. McDaniel, Identification and Correction of Axial Force Prediction Discrepancies due to Angle of Attack Effects in Missile Datcom, AIAA-2005-4833, 2005.
- [8] Christopher Rosema, Mark Underwood and Lamar Auman, Recent Fin Related Improvements for Missile Datcom, AIAA-2007-3937, 2007.

THIS PAGE INTENTIONALLY LEFT BLANK

INITIAL DISTRIBUTION LIST

1. Defense Technical Information Center
Ft. Belvoir, VA
2. Dudley Knox Library
Naval Postgraduate School
Monterey, CA
3. Professor M. S. Chandrasekhara
Department of Mechanical and Astronautical Engineering
NASA Ames Research Center, M.S. 215-1
Moffett Field, CA
4. Robert L. Dewitt
Defense Intelligence Agency
Missile & Space Intelligence Center, MSD-2/ Dewitt
Redstone Arsenal, AL
5. Jay A. Witt
Defense Intelligence Agency
Missile & Space Intelligence Center
Redstone Arsenal, AL
6. Lamar M. Auman
Chief – Aerodynamic Technology
U.S. Army AMRDEC
AMSRD-AMR-SS-AT
Redstone Arsenal, AL
7. Professor Yeo Tat Soon, Director
Temasek Defence Systems Institute
National University of Singapore
Singapore
8. Tan Lai Poh (Ms), Assistant Manager
Temasek Defence Systems Institute
National University of Singapore
Singapore